I&EC research
Industrial & Engineering Chemistry Research

pubs.acs.org/IECR

Article

Effects of Concentration Polarization and Membrane Orientation on the Treatment of Naproxen by Sulfate Radical-Based Advanced Oxidation Processes within Nanofiltration Membranes with a Catalytic Support

Tao Wang, Joris de Grooth, and Wiebe M. de Vos*

Cite This: *Ind. Eng. Chem. Res.* 2023, 62, 7622−7634

Read Online

ACCESS | Metrics & More | Article Recommendations | Supporting Information

ABSTRACT: The structure with a selective nanofiltration (NF) layer on top of a catalytic ultrafiltration (UF) membrane provides the possibility of treating micropollutants (MPs) by both rejection and degradation. However, such a dense selective layer unavoidably induces a formation of a highly concentrated retentate and a low utilization of the oxidant due to its rejection. A different membrane orientation is expected to solve the problems mentioned above since the concentrated MPs can be degraded within the catalytic support, and the rejection of the oxidants can be avoided when the pressure is applied from the porous support side. However, the resulting complex concentration polymerization (CP) effects are not well understood, and the effects of the following concentration changes of the MPs and the oxidants around the catalyst within the porous support membrane are unclear as well. In this work, three polyelectrolyte multilayers with different selectivity were fabricated on PES@$CoFe_2O_4$ catalytic UF membranes by sequential dip-coating. Concentration polarization models are utilized to predict the concentrations of naproxen and peroxymonosulfate (PMS) within the porous catalytic support under different membrane orientations. The results of naproxen removal after adding PMS show that a higher naproxen removal can be obtained with a higher concentration ratio of PMS to naproxen (c_{PMS}/c_{NPX}). Moreover, it is shown that the MPs in the feed solution can be degraded in a catalysis-separation sequence, exhibiting the potential of rejecting and simultaneously degrading MPs. However, the coating of a selective polyelectrolyte multilayer on the catalytic UF membranes also causes lower accessibility of PMS and naproxen to the catalysts embedded within the polymeric membranes, resulting in the decline of degradation efficiency. By coating only one side of the membranes, this negative effect caused by the polyelectrolyte coating can be mitigated. Overall, a 97% removal of naproxen on the permeate side and a 12% degradation of naproxen on the feed side were observed with the one-side-coated membranes under a catalysis-separation sequence. This work highlights the key role that concentration polarization can play in the degradation efficiency of naproxen in catalytic NF membranes, providing valuable guidance for the design of further improved catalytic membranes.

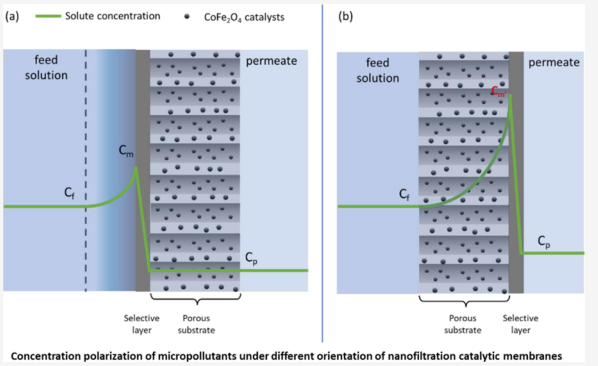

Concentration polarization of micropollutants under different orientation of nanofiltration catalytic membranes

1. INTRODUCTION

Due to their high efficiency in degrading small organic micropollutants (MPs), sulfate radical-based advanced oxidation processes (SR-AOPs) are regarded as a promising technique in the treatment of MP-containing wastewaters, such as municipal wastewater.[1−3] Singlet oxygen (non-radical pathways) and reactive radicals, including sulfate radicals and hydroxyl radicals, can be easily generated in SR-AOPs by activating peroxymonosulfate (PMS) or peroxydisulfate (PDS), leading to the degradation of MPs to byproducts or CO_2 and water.[4−6] To activate PMS or PDS, heterogeneous catalysts have drawn more attention compared to homogeneous metal ions because the former overcome the downside of high concentrations of metal ions leaching into the effluent.[7] However, the use of heterogeneous catalysts also faces difficulties, for example, in mass transfer limitation and in reusing and recycling these small-sized catalysts.[8,9] Even though some of the heterogeneous magnetic catalysts can be separated by a magnetic field,[10−12] the aggregation of the small-sized catalysts is still unavoidable in this process, resulting in a decline in their activation efficiency.

Recently, the development of SR-AOP-based catalytic membranes has provided an alternative method to treat MPs

Received: February 24, 2023
Revised: April 19, 2023
Accepted: April 25, 2023
Published: May 4, 2023

https://doi.org/10.1021/acs.iecr.3c00592
Ind. Eng. Chem. Res. 2023, 62, 7622−7634

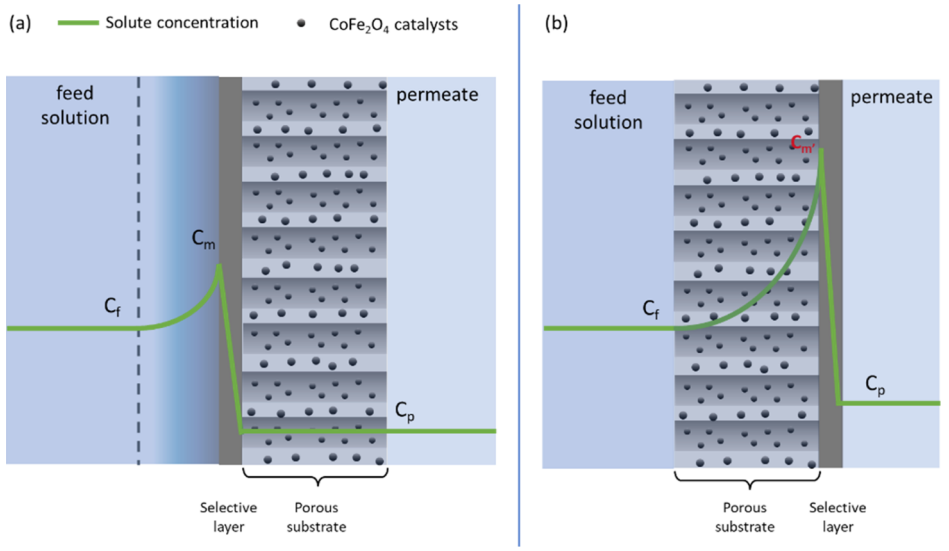

Figure 1. Schematic graph of concentration polarization profiles under two different membrane orientations: (a) SL-F and (b) SL-P.

in wastewater, showing great potential in achieving a synergistic effect of membrane separation and AOPs.[13−15] By embedding catalysts into the membrane structure, the difficulties in reusing and recycling the small-sized catalysts can be circumvented.[16] Meanwhile, when the catalysts are immobilized in the porous membrane structure, not only the MP removal can be enhanced due to the degradation via AOPs, but also, the flow applied in the membrane separation process significantly enhances the contact of the reactants and reduces the mass transport resistance, boosting the degradation of MPs.[17,18] Currently, most of the reported SR-AOP-based catalytic membranes are within the microfiltration (MF) or ultrafiltration (UF) range. Compared with denser nanofiltration (NF) membranes, the relatively lower operating energy is the strength of the MF or UF membranes.[19] However, it also means that these porous membranes cannot function as a separation barrier for MPs, which means that the membranes cannot contribute to the removal of MPs. To design a dense catalytic membrane, which provides sufficient rejection to MPs, the position of immobilizing catalysts in the membrane structure is important. Normally, immobilizing catalysts in the porous support membrane are favored compared with fixing catalysts on top of or within the selective layer. As the selective layer is very thin, there would be a too short residence time with the same flux, insufficient catalyst loading, and a too high mass transfer resistance for it to function effectively as a catalyst support.[20]

In our previous work, the catalyst $CoFe_2O_4$ was embedded within the porous support membrane by blending the catalyst with polyethersulfone (PES), after which a polyelectrolyte multilayer was coated on top of the catalytic support.[19] The obtained NF catalytic membranes exhibited both rejection and degradation toward naproxen. However, the structure of this dense catalytic membrane, having a selective layer on top of the catalytic support, still induces several problems. As the selective layer rejects not only MPs but also the oxidant (PMS), only part of the PMS can reach the porous support where the catalysts are immobilized, lowering the utilization of PMS. Meanwhile, due to the rejection of MPs, the highly concentrated retentate still needs a post-treatment.

To solve the problems, membrane orientation becomes an interesting parameter that could be utilized when the catalytic NF membranes with an asymmetric structure are applied. In a normal operation, one would have a dense separation layer before the catalytic support, but it is also possible to invert the operation and have the catalytic degradation before the separation layer (see Figure 1). In this case, all the added PMS can first contact the catalysts embedded within the porous support rather than the selective layer and thus be 100% utilized for the AOP. Besides, as the concentrated MPs within the porous support can be degraded by the AOP, the concentrated retentate is expected to be strongly reduced, and the post-treatment of highly concentrated MPs can be avoided. As such, it could be very interesting to invert the membrane orientation, leading to catalytic first and membrane rejection second. However, due to the accumulation of solutes within the porous support membrane, a severe internal concentration polarization (ICP) can be induced by the invert of membrane orientation, which influences the concentrations of MPs and oxidants around the catalysts. It has been widely reported that the reaction kinetics of SR-AOPs are highly dependent on the concentrations of reactants. Within a certain concentration range, a higher concentration of oxidants results in better removal of MPs with a fixed concentration of MPs, while a higher concentration of MPs shows the opposite effect.[21−23] Thus, the concentrations of both oxidants and MPs within the porous catalytic support membrane will be determining factors for the degradation efficiency of MPs by catalytic membranes. Moreover, the effects of concentration polarization will be very different for different catalytic membrane orientations. In the separation-catalysis sequence, both the concentrations of MPs and oxidants would drop after the selective layer. However, the concentration ratio between MPs and oxidants could be significantly altered due to differences in rejection. When the catalysis process is followed by membrane separation, both MPs and oxidants would be concentrated within the porous catalytic support due to the existence of the selective layer. In this case, a much more severe concentration polarization occurs within the porous support membranes since the concentrated solutes within the porous support cannot be well-mixed with the feed solution. Therefore, similar to the

https://doi.org/10.1021/acs.iecr.3c00592
Ind. Eng. Chem. Res. 2023, 62, 7622−7634

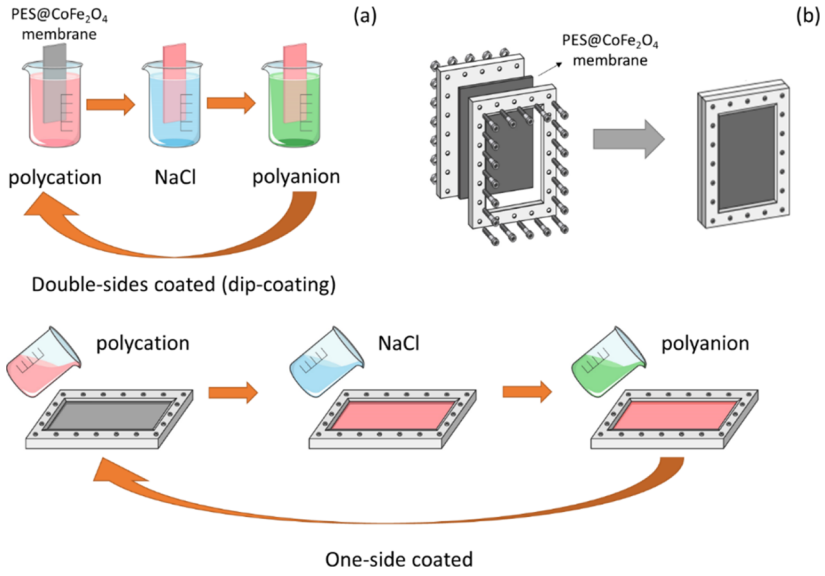

Figure 2. Schemes of the methods used to build polyelectrolyte selective layers on top of the UF catalytic membranes containing $CoFe_2O_4$ catalysts ($PES@CoFe_2O_4$): (a) double-side-coated (dip-coating method) and (b) one-side-coated.

forward osmosis process, the concentrations of MPs and oxidants are not only influenced by the rejection ability of the selective layer but also by the structural parameter of the porous catalytic support membranes.[24,25] With different concentration polarization moduli of MPs and oxidants, MPs and the oxidants exhibit different enrichment factors, which will affect the degradation efficiency within the catalytic support membranes. Little work has been done to explore the concentrations of MPs and oxidants within the porous catalytic support for different membrane orientations, and we lack a comprehensive understanding of the effects of concentration polarization on MP degradation when a selective layer is combined with a catalytic support membrane.

In this work, PMS was chosen as the representative oxidant. Naproxen was chosen as a representative MP since it has been extensively used as a non-selective, non-steroidal, and anti-inflammatory drug and has been widely detected in not only wastewater but also groundwater and surface water.[26] The catalytic support membranes were fabricated by the method that we used in our previous work, in which the catalyst $CoFe_2O_4$ was blended with PES as the casting solution, and non-solvent-induced phase inversion was used to fabricate the membranes.[19] On top of the catalytic support membranes, three types of polyelectrolyte multilayers with different rejection behaviors were produced following the work of te Brinke et al.[27] Two methods for fabricating the selective layers, including dip-coating and one-side coating, were applied as shown in Figure 2. To investigate the influence of the catalysis-separation order, all the membranes were measured in two different membrane orientations, which are selective layer faces feed solution (SL-F) and selective layer faces permeate (SL-P). The $MgSO_4$ rejections measured in SL-F and SL-P modes were fitted into concentration polarization models to obtain structural parameters of the membranes, which were then applied to estimate the concentrations of PMS and naproxen within the porous catalytic support. The removals of naproxen before and after adding PMS were measured in SL-F and SL-P modes to show the treatment efficiency. Meanwhile, the possibility of degrading naproxen in the retentate under the SL-P mode was also explored. This work systematically investigated the effects of concentration polarization on the degradation efficiency of naproxen by analyzing the concentrations of naproxen and PMS within the catalytic support. The significant role of concentration polarization under different membrane orientations in the degradation efficiency of naproxen is revealed, giving important insights into the design of catalytic membranes with a dense selective layer.

2. THEORY

2.1. Description of External Concentration Polarization When the Selective Layer Faces the Feed. Figure 1a shows the concentration profiles across an asymmetric membrane when the membrane is measured in the SL-F mode. In the SL-F mode, the solute concentration within the boundary layer (c_m, mol/m^3) can be correlated to the solute concentration in the feed solution (c_f, mol/m^3) and the permeate (c_p, mol/m^3) using eq 1[28]

$$\frac{c_m - c_p}{c_f - c_p} = \exp^{(J_w/k)} \tag{1}$$

where J_w (m/s) is the water flux and k (m/s) is the mass transfer coefficient. To obtain the mass transfer coefficient, the average Sherwood number ($\overline{Sh}$) as a function of the Reynolds number and Schmidt number for the rectangular cross-flow setup is used here[29]

$$\overline{Sh} = 1.85(Re\ Sc\ de/L)^{1/3} = k\ de/D \tag{2}$$

where de (m) is the equivalent hydraulic diameter, which is 4 times higher than the half-channel height of the membrane chamber, and L (m) is the channel length. Re and Sc are the Reynolds number and Schmidt number, which can be defined, respectively, as

$$Re = \rho u_0 de/\mu \tag{3}$$

$$Sc = \mu/\rho D \tag{4}$$

where ρ (kg/m^3) is the density of the solution, u_0 (m/s) is the average bulk velocity, μ (Pa s) is the viscosity of the solution, and D (m^2/s) is the diffusivity coefficient. The diffusion

https://doi.org/10.1021/acs.iecr.3c00592
Ind. Eng. Chem. Res. 2023, 62, 7622−7634

coefficient of different solutes used in this work can be found in Text S1. By integrating 2, the following equation of k can be obtained

$$k = 1.85(u_0 D^2/de/L)^{1/3} \quad (5)$$

With the value of k, the concentration within the boundary layer can be obtained based on eq 1. The external concentration polarization modulus (ECP modulus) is calculated by the concentration ratio of c_m and c_f,[30] which is

$$\text{ECP modulus} = c_m/c_f \quad (6)$$

2.2. Description of Internal Concentration Polarization When the Selective Layer Faces the Permeate. As shown in Figure 1b, the ICP occurs within the porous support membranes in the SL-P mode. The flux of the solute, J_s (mol m^{-2} s^{-1}), across the separation layer can be written as[31]

$$J_s = B\cdot(c_{m'} - c_p) = J_w\cdot c_p \quad (7)$$

where B (m/s) is the solute permeation coefficient of the membrane and $c_{m'}$ (mol/m^3) and c_p (mol/m^3) are the concentrations of the solute at the interface of the support and selective layer and in the permeate, respectively. Within the porous support membranes, the solute permeation consists of two parts, which are the advective transport of solutes due to the water flux and diffusive transport of solutes, in the opposite direction, according to a concentration boundary layer build-up caused by the membrane retention. Thus, the transport of the solutes within the porous support can also be written as[32]

$$J_s = -D\cdot p\cdot\frac{dc(x)}{dx} + J_w\cdot c(x) \quad (8)$$

where p is the porosity of the substrate and x (m) is the distance from the membrane−solution interface to the porous support membranes. By combining eqs 7 and 8, eq 9 can be obtained

$$B\cdot(c_{m'} - c_p) = -D\cdot p\cdot\frac{dc(x)}{dx} + J_w\cdot c(x) \quad (9)$$

The concentrations at the boundary are

$$c(x) = c_f, \quad \text{at } x = 0$$

$$c(x) = c_{m'}, \quad \text{at } x = \tau\cdot t$$

where τ and t (m) are the tortuosity and thickness of the support membrane, respectively. By integrating the boundary conditions with eq 9, the concentration of the solute within the porous support can be derived as

$$c_{m'} = (c_f - c_p)\times \exp^{J_w\cdot S/D} + c_p \quad (10)$$

where S is the structural parameter of the porous support membranes, which is defined as[31]

$$S = \frac{\tau\cdot t}{p} \quad (11)$$

To measure the structural parameters of membranes with different selectivities, the rejections (R) of membranes under different fluxes were measured under different membrane orientations based on eq 12

$$R = 1 - \frac{c_p}{c_f} \quad (12)$$

To obtain permeability coefficient (B) of the solutes, eq 13 from the literature was utilized, and the rejections (R) measured in the SL-F mode as a function of fluxes (J_w) were fitted into eq 13[33]

$$R = \frac{k - J_w}{k\left(\frac{B}{J_w} + 1\right) - J_w} \quad (13)$$

Furthermore, eq 14 can be derived as follows by integrating eq 12 with eq 10

$$R = \frac{J_w/B}{\exp^{J_w\cdot S/D} + J_w/B} \quad (14)$$

By applying B to eq 14, the structural parameters of the membranes with different selectivities can be obtained by fitting the rejections at different fluxes measured in the SL-P mode in eq 14. With the structural parameters of the membranes, the concentration of the solute within the porous support can be calculated based on eq 10. Similar to the calculation of the ECP modulus, the ICP (ICP modulus) is calculated by the concentration ratio of $c_{m'}$ and c_f, which is

$$\text{ICP modulus} = c_{m'}/c_f \quad (15)$$

3. MATERIALS AND METHODS

3.1. Chemicals. PES (Ultrason 6020) and sulfonated PES (SPES) (Ultrason 0559) were obtained from BASF. Cobalt iron oxide nanopowder (30 nm), glycerol (≥99.5%), oxone ($KHSO_5\cdot 0.5KHSO_4\cdot 0.5K_2SO_4$, mono persulfate compound), poly(diallyldimethylammonium chloride) (PDADMAC, 200−350 kDa, 20 wt % in water), poly(styrenesulfonate) (PSS, 200 kDa, 30 wt % in water), $Na_2B_4O_7\cdot 10H_2O$, H_3BO_3, and naproxen ($C_{14}H_{14}O_3$, M_w: 230.26 g/mol) were purchased from Sigma-Aldrich. Poly(allylamine hydrochloride) (PAH, 150 kDa, 40 wt % in water) was obtained from Nittobo Medical, Japan. Glutaraldehyde (25 wt % in water) was obtained from Alfa Aesar-Thermo Fisher. Potassium iodide (KI, 166 g/mol) was purchased from Acros Organics-Thermo Fisher. All the chemicals were used without further purification steps.

3.2. Membrane Fabrication. The UF catalytic membranes were fabricated following the method developed in a previous study, and the characterization of UF membranes by scanning electron microscopy, energy-dispersive X-ray spectroscopy, X-ray photoelectron spectroscopy, and X-ray fluorescence can be found therein.[19] Briefly, 1.0 wt % $CoFe_2O_4$ catalysts, 14 wt % PES, 7.0 wt % SPES, and 12 wt % glycerol were first dissolved in N-methylpyrrolidone. The obtained casting solution was cast by a casting knife with a gap height of 150 μm and then put into a Milli-Q water coagulation bath. On top of the obtained UF catalytic membranes, layer-by-layer assembly of polyelectrolytes was conducted to build separation layers. Two coating methods were applied in this work, which are dip coating (which coats both sides) and one-sided coating. As shown in Figure 2a, the dip-coating process was performed by alternatively putting membrane samples into the solutions of polycations and polyanions (0.1 g/L, dissolved in 500 mM NaCl) for 15 min. After each coating step, the membranes were rinsed with a 500 mM NaCl background solution three times to get rid of the loosely bounded polyelectrolytes. One bilayer can be obtained by coating one layer of polycations and subsequently one layer of polyanions. In this work, PDADMAC and PAH were used

https://doi.org/10.1021/acs.iecr.3c00592
Ind. Eng. Chem. Res. 2023, 62, 7622−7634

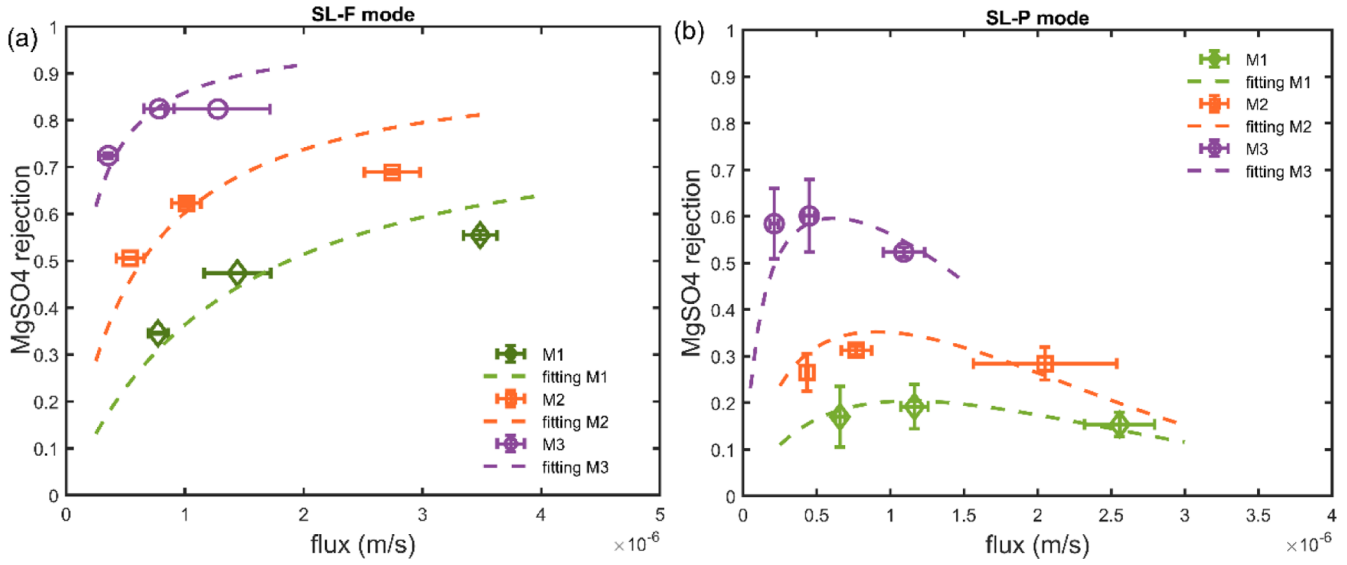

Figure 3. $MgSO_4$ rejections as a function of membrane flux under different membrane orientations: (a) SL-F mode and (b) SL-P mode. Data in SL-F and SL-P modes were fitted with eqs 13 and 14, respectively. The pressures applied in this measurement were 0.5, 1.0, and 2.0 bar. The cross-flow velocity was 0.077 m/s. For every data point, three individual membrane samples are measured, and errors are given as the standard deviation.

as polycations, and PSS was used as the polyanion. The UF catalytic support membranes are denoted M_0. On top of M_0, 7.0 bilayers of PDADMAC and PSS were coated, and the obtained membranes are denoted M_1. On top of M_1, 4.5 bilayers of PAH and PSS were coated to obtain a membrane with asymmetric polyelectrolyte multilayers (M_2). To further increase the selectivity of M_2, the outmost PAH layers were cross-linked with 7.5 mM glutaraldehyde, and the obtained membranes were denoted M_3. In this dip-coating method, both sides of the membranes were coated with polyelectrolytes. To explore the effect of coating on the accessibility of reactants to the catalysts within the porous support, the one-side coating method was also used as shown in Figure 2b. 80 mL of polyelectrolyte solution was poured into the setup to start the coating process, and after 15 min, 80 mL of NaCl solution (500 mM NaCl) was used to rinse the membrane three times between the polyelectrolyte coatings. The polyelectrolytes used in the one-side coating are the same as those used in the dip-coating methods.

3.3. $MgSO_4$ Rejection. To determine the structural parameters of different membranes, $MgSO_4$ was chosen as the model solute based on the following reasons: first, PMS contains SO_4^{2-} ions, and they would be generated after the activation as well; second, Mg^{2+} ions were chosen as the cations instead of K^+ ions because it is easier to see a difference on the Mg^{2+} rejection for the membranes fabricated with different selectivities; moreover, Mg^{2+} is also a typical divalent cation, which has widely been used in the rejection measurement of membranes.[34] The $MgSO_4$ rejections of M_1, M_2, and M_3 were measured in both SL-F and SL-P modes. A cross-flow setup (CF 042, Sterlitech) with a membrane area of 42 cm^2 was used, and different pressures (1.0, 2.0, and 3.0 bar) were applied for this measurement. 1 L of $MgSO_4$ (5 mM) solution was used as the feed solution. The membranes were first pre-compacted at the target pressure for 30 min. After this, $MgSO_4$ solutions from both the feed and permeate sides were collected. The concentrations of $MgSO_4$ solutions were measured by a conductivity meter (CondTM 3210, WTW). The rejection was calculated based on eq 12. Meanwhile, the weight of the permeates was also monitored in 15 min time intervals, and the membrane flux (J_w, m/s) was calculated following eq 16

$$J_w = \frac{V}{A\Delta t} \tag{16}$$

where V (m^3) is the permeate volume, A (m^2) is the membrane area, and Δt (s) is the permeation time.

3.4. Naproxen Rejection. Naproxen with a concentration of 2 mg/L (8.7 μmol/L) was chosen as the model MP, and rejections of naproxen were measured in the same crossflow setup that was used for the $MgSO_4$ rejection measurement. $Na_2B_4O_7{\cdot}10H_2O$ (2.5 mM) and H_3BO_3 (10 mM) were used as a buffer to control the pH of the naproxen solution at around 7.8.[35,36] As the flux in the membrane-catalysis process plays an important role, affecting the residence time during the catalytic reactions,[19,37] the pressures applied for membranes with different selectivities were adjusted to make sure that all the membranes were operated at the same flux (4 ± 0.5 L/m^2/h). The fluxes of different membranes during the naproxen rejection measurement are shown in Figure S1. In a typical measurement, the membranes were first permeated at the target flux with 1 L of naproxen solution for 24 h to reach an adsorption−desorption equilibrium. During this process, all the permeates were recycled back into the feed solution. After this, the permeate and feed solutions were collected, and the initial naproxen rejection without catalytic reactions can be calculated based on eq 12. The catalytic reactions start with the addition of 2 mL of a PMS stock solution (500 mM) to achieve a PMS concentration of 1 mM. As it takes some time for the old permeate to be fully removed, 0.8 mL naproxen solution samples were taken after 75, 90, 105, and 120 min from both the feed and permeate sides. Immediately, 0.2 mL of methanol was added to the samples to quench the catalytic reactions.[38] The concentrations of naproxen samples were measured by high-performance liquid chromatography (Dionex Ultimate 3000), and the details of the column, mobile phase, and UV detector can be found in our previous work.[19,27] The rejection of naproxen after adding PMS was calculated

https://doi.org/10.1021/acs.iecr.3c00592
Ind. Eng. Chem. Res. 2023, 62, 7622−7634

following eq 12 as well. The removal of naproxen was calculated using eq 17

$$\text{removal} = \left(1 - \frac{c_p}{c_0}\right) \times 100\% \tag{17}$$

where c_0 (mol/m^3) is the concentration of the initial naproxen solution.

3.5. PMS Rejection. Because PMS would be activated with the occurrence of catalytic membranes, the catalytic membranes cannot be directly used to measure the rejection of PMS. In this experiment, control membranes were used to measure the rejection of PMS, and the same selective layers were fabricated on top of the control UF membranes without the $CoFe_2O_4$ catalyst by the dip-coating method. The concentration of PMS in the feed solution was 1 mM. The pressure was adjusted to the same pressure used in the naproxen rejection measurement to make sure that the fluxes were the same for membranes with different selectivity. The concentration of PMS was measured following the method in the work of Liang et al.[39] Briefly, 0.5 mL of KI solution (0.4 g/mL) and 0.5 mL of $NaHCO_3$ (0.02 g/mL) were added to 1 mL of PMS solutions. After 15 min, 1 mL of the obtained solution was diluted 10 times with Milli-Q water. Subsequently, a UV−vis spectrophotometer (UV-1800, Shimadzu Corporation, Japan) was used to measure the adsorption at 352 nm. The calibration curve of the PMS rejection measurement is shown in Figure S2. The rejection of PMS was calculated based on eq 12.

4. RESULTS AND DISCUSSION

4.1. Determining the Structural Parameter (S) of the Membranes. As elaborated in the theoretical section, the structural parameters (S) of membranes with different selectivity are needed to calculate the concentrations of solutes within the porous support in the SL-P mode. In this work, membranes with different selectivity were obtained by coating a polyelectrolyte multilayer on top of a catalytic support (M_0). M_1 was coated with 7.0 bilayers of PDADMAC and PSS. An extra 4.5 bilayers of PAH and PSS were coated on top of M_1 to obtain a membrane with asymmetric polyelectrolyte multilayers (M_2). M_3 was obtained by crosslinking M_2 with 7.5 mM glutaraldehyde. $MgSO_4$ was used as the model solute, and the rejections of $MgSO_4$ under different fluxes were measured in both SL-F and SL-P modes to obtain the values of S for M_1, M_2, and M_3.

As shown in Figure 3, the $MgSO_4$ rejections of M_3 are higher than the rejections of M_1 and M_2 in both SL-F and SL-P modes, indicating that the selectivity of the membrane increases with more polyelectrolyte layers and cross-linking. Moreover, Figure 3a shows the fitting of the $MgSO_4$ rejections in the SL-F mode as a function of fluxes into eq 13. The $MgSO_4$ permeability (B) of M_1, M_2, and M_3 can be obtained from the fitting, which is listed in Table 1. Subsequently, the obtained values of B were applied to eq 14. By fitting the $MgSO_4$ rejections at different fluxes measured in the SL-P mode in eq 14 as shown in Figure 3b, the structural parameters of the membranes with different selectivity can be obtained. Table 1 lists the structural parameters of M_1, M_2, and M_3 obtained based on the $MgSO_4$ rejection measurement, which can be then used to calculate the expected concentrations of naproxen and PMS within the porous part of the membranes based on eq 10. Moreover, it can be observed from the results of structural parameters that the value of S increases from 0.7 mm of M_1 to 1.2 mm of M_3, although all the membranes were fabricated on the same support. Similar results were also obtained in the work of Reurink et al., where the structural parameters were different when different polyelectrolyte pairs were coated on the same support.[40] A possible explanation is that the inside of the support is also coated with the polyelectrolyte, which influences the transport in the support. Besides, the limitation of this simplified model can also be the reason because the ECP is neglected when ICP is discussed, which also affects the estimation of structural parameters.

Table 1. $MgSO_4$ Permeability and Structural Parameters of Different Membranes

membrane type	B^a ($MgSO_4$ permeability, m/s)	S^a (structural parameter, mm)
M_1	1.6^{-6}	0.7
M_2	6.1^{-7}	0.8
M_3	1.5^{-7}	1.2

[a]The 95% confidence intervals of B and S can be found in Table S1.

4.2. Effect of CP on Naproxen Degradation. When the membrane separation is solely used to treat wastewater containing MPs, the rejection of MPs results in an increase of MPs near the membrane surface, and then, a boundary layer forms, which causes concentration polarization. Concentration polarization normally exhibits negative effects on selectivity and membrane flux.[30] In an AOP-coupled-separation process, besides the effects on the membrane separation performance, concentration polarization is also expected to influence the degradation efficiency of MPs because the reaction kinetics of radical generation and MP degradation are highly affected by the concentrations of the MPs and oxidants near the catalysts. In this work, the effects of MPs and oxidant concentration variation induced by concentration polarization are explored, and naproxen and PMS are chosen as the model MP and oxidant, respectively.

The rejections of naproxen and PMS are first measured when there are no catalytic reactions. As shown in Figure 4a, the naproxen rejections measured in the SL-F mode are all higher than those in the SL-P mode because the ICP that occurs in the SL-P mode is much more severe than the ECP in the SL-F mode.[24] For the same reason, the rejections of PMS in the SL-P mode, as shown in Figure 4b, exhibit a similar trend when compared to the rejections of PMS in the SL-F mode. Meanwhile, it can be observed that the rejections of PMS are much lower than the rejections of naproxen and even $MgSO_4$ (Figure 3), which can be attributed to the smaller molecule size of PMS compared to that of naproxen and the PMS counterion K^+ compared to Mg^{2+}. Among all the membranes fabricated, M_3 exhibited the highest naproxen rejection in both SL-F and SL-P modes, indicating again that the crosslinking between PAH and GA makes the selective layer much denser.[27] Although M_2 possesses an extra 4.5 bilayers of PAH/PSS compared with M_1, there is not a big improvement in the rejections of both naproxen and PMS, which corresponds to the results of $MgSO_4$ rejections. With the rejections of naproxen and PMS by only membrane separation, the concentration moduli of different membranes in both SL-F and SL-P modes can also be calculated based on the theory section, which are shown in Figure 4c,d. From M_1 to M_3, the concentration polarization moduli in both SL-F and SL-P modes gradually increase, resulting from the increased

https://doi.org/10.1021/acs.iecr.3c00592
Ind. Eng. Chem. Res. 2023, 62, 7622−7634

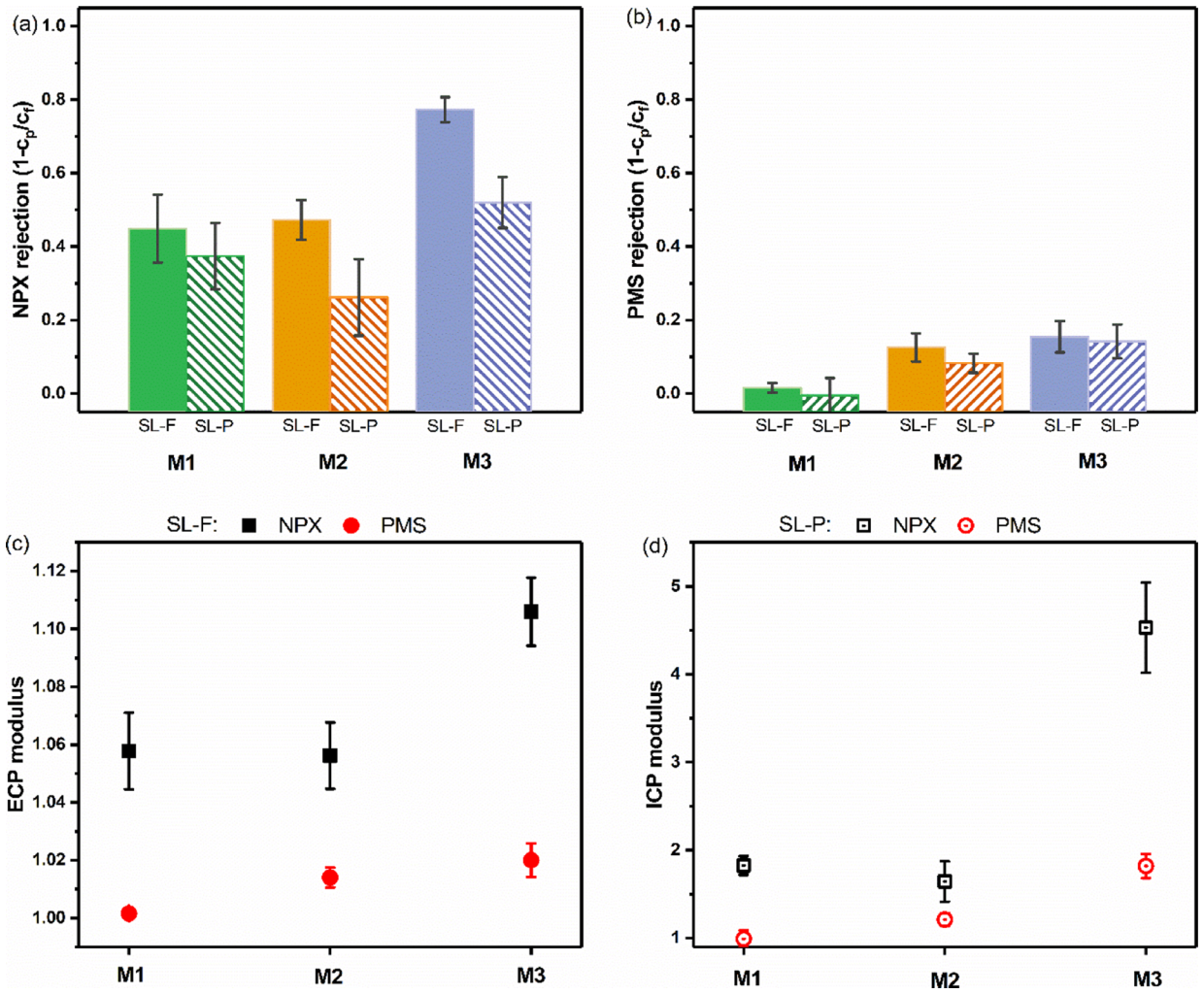

Figure 4. Rejections of naproxen and PMS and the concentration polarization moduli of M_1, M_2, and M_3 in the SL-F mode and SL-P mode: (a) rejections of naproxen measured without adding PMS; (b) rejections of PMS measured by control membranes with the same selective layers; (c) concentration polarization moduli of naproxen and PMS in the SL-F mode; and (d) concentration polarization moduli of naproxen and PMS in the SL-P mode. To ensure the same residence time, all the membranes were measured under the same flux, which can be found in Figure S1. The pressures applied in naproxen rejection for M_1, M_2, and M_3 were 0.75 ± 0.17 bar, 1.06 ± 0.14 bar, and 2.0 ± 0.18 bar, respectively, in the SL-F mode and 1.37 ± 0.2 bar, 1.5 ± 0.18 bar, and 2.6 ± 0.32 bar, respectively, in the SL-P mode. The pressures applied in PMS rejection for M_1, M_2, and M_3 were 0.69 ± 0.04 bar, 1.14 ± 0.05 bar, and 1.6 bar, respectively, in the SL-F mode and 1.11 ± 0.16 bar, 1.19 ± 0.16 bar, and 2.17 ± 0.24 bar, respectively, in the SL-P mode. The cross-flow velocity was 0.077 m/s. For every data point, three individual membrane samples are measured, and errors are given as the standard deviation.

selectivity of the membranes. Not surprisingly, the ICP moduli measured in the SL-P mode are much higher than those of ECP in the SL-F mode due to the ICP that occurs within the porous support.

Since the reactions of SR-AOPs occur within the porous support membrane where the catalysts are embedded, the concentrations of naproxen and PMS within the porous support are expected to show effects on the degradation efficiency. In the SL-F mode, the concentrations of naproxen and PMS within the porous support can be easily calculated from the concentration in the permeate based on the assumption that no concentration polarization occurs on the permeate side of the membranes. Meanwhile, the concentrations of naproxen and PMS within the porous support in the SL-P mode can also be calculated based on eq 10. Naturally, we are aware that these concentrations will change when a catalytic process is taking place. However, as elaborated in the introduction, both the initial concentrations of MPs and the oxidant influence the eventual removal of MPs in the batch experiment. The initial concentrations of naproxen and PMS within the catalytic porous support are thus expected to work as a useful indicator to estimate the reaction kinetics of catalytic reactions in AOPs.

The concentrations of naproxen and PMS within the porous support are shown in Figure S3. In the SL-F mode, the concentrations of naproxen and PMS are both lower than the initial concentrations added, while the concentrations in the SL-P mode exhibit the opposite change. Considering this opposite concentration variation under different membrane orientations, it is difficult to compare the effect of membrane orientation with that of the absolute concentrations of naproxen and PMS. Therefore, the concentration ratio between PMS and naproxen ($R_{PMS/NPX}$) within the porous support is used here to solve this problem, which is calculated based on eq 18

https://doi.org/10.1021/acs.iecr.3c00592
Ind. Eng. Chem. Res. 2023, 62, 7622−7634

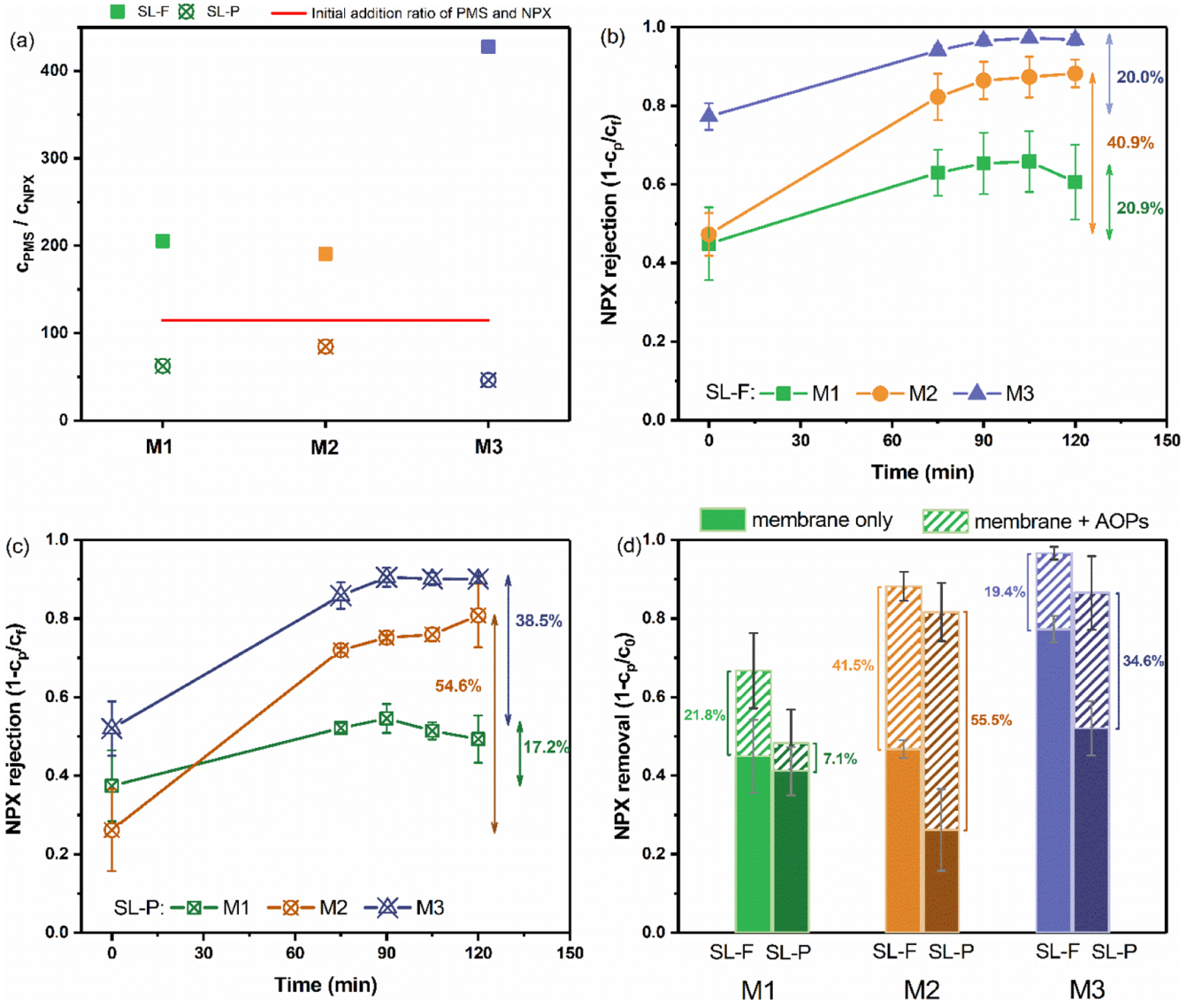

Figure 5. Treatment efficiency of naproxen with the addition of PMS in a cross-flow setup: (a) ratios of PMS and naproxen concentrations within the porous support in the SL-F mode and SL-P mode, as calculated by c_{PMS}/c_{NPX}. The concentrations of both naproxen and PMS within the porous support were measured or calculated based on the individual measurements of PMS and naproxen. (b) Naproxen rejection before and after adding PMS in the SL-F mode (the rejection at 0 min represents the initial rejection by only the membranes, and PMS was added after 0 min); (c) naproxen rejection before and after adding PMS in the SL-P mode; and (d) naproxen removal before and after adding PMS under different membrane orientations. Since PMS was added after the measurement of naproxen rejection, the pressures applied in naproxen rejection with PMS addition were the same as those in Figure 4, which were 0.75 ± 0.17 bar, 1.06 ± 0.14 bar, and 2.0 ± 0.18 bar for M_1, M_2, and M_3, respectively, in the SL-F mode and 1.37 ± 0.2 bar, 1.5 ± 0.18 bar, and 2.6 ± 0.32 bar for M_1, M_2, and M_3, respectively, in the SL-P mode. The cross-flow velocity was 0.077 m/s. For every data point, three individual membrane samples are measured, and errors are given as the standard deviation.

$$R_{PMS/NPX} = c_{PMS}/c_{naproxen} \quad (18)$$

where c_{PMS} and $c_{naproxen}$ are the concentrations of PMS and naproxen within the porous catalytic support, respectively. As it has been reported that within a certain concentration range, a higher percentage of MPs can be removed in a batch experiment when a higher concentration of oxidants is added into a fixed concentration of MPs or when a lower concentration of MPs is treated with a fixed concentration of PMS,[21−23,41] a higher value of $R_{PMS/NPX}$ is expected to boost the removal efficiency of naproxen.

As shown in Figure 5a, the initial addition ratio between PMS (1000 μmol/L) and naproxen (8.7 μmol/L) is 115, which is represented by the red line. For the three types of membranes with different selectivity to naproxen and PMS, $R_{PMS/NPX}$ are all higher than the initial addition ratio in the SL-F mode while lower than the initial addition ratio in the SL-P mode. PMS and naproxen are both rejected by the selective layer in the SL-F mode. However, due to the relatively low PMS rejection compared with naproxen rejection, more PMS molecules permeate through the selective layer than naproxen, and thus, $R_{PMS/NPX}$ in the SL-F mode are higher than the initial addition ratio, while in the SL-P mode, a lower PMS rejection means that the enrichment of PMS is much less than that of naproxen. Therefore, the difference in membrane orientations leads to an opposite effect on the $R_{PMS/NPX}$ within the porous support membranes, which are expected to further affect the degradation efficiency of naproxen in catalytic membranes.

https://doi.org/10.1021/acs.iecr.3c00592
Ind. Eng. Chem. Res. 2023, 62, 7622−7634

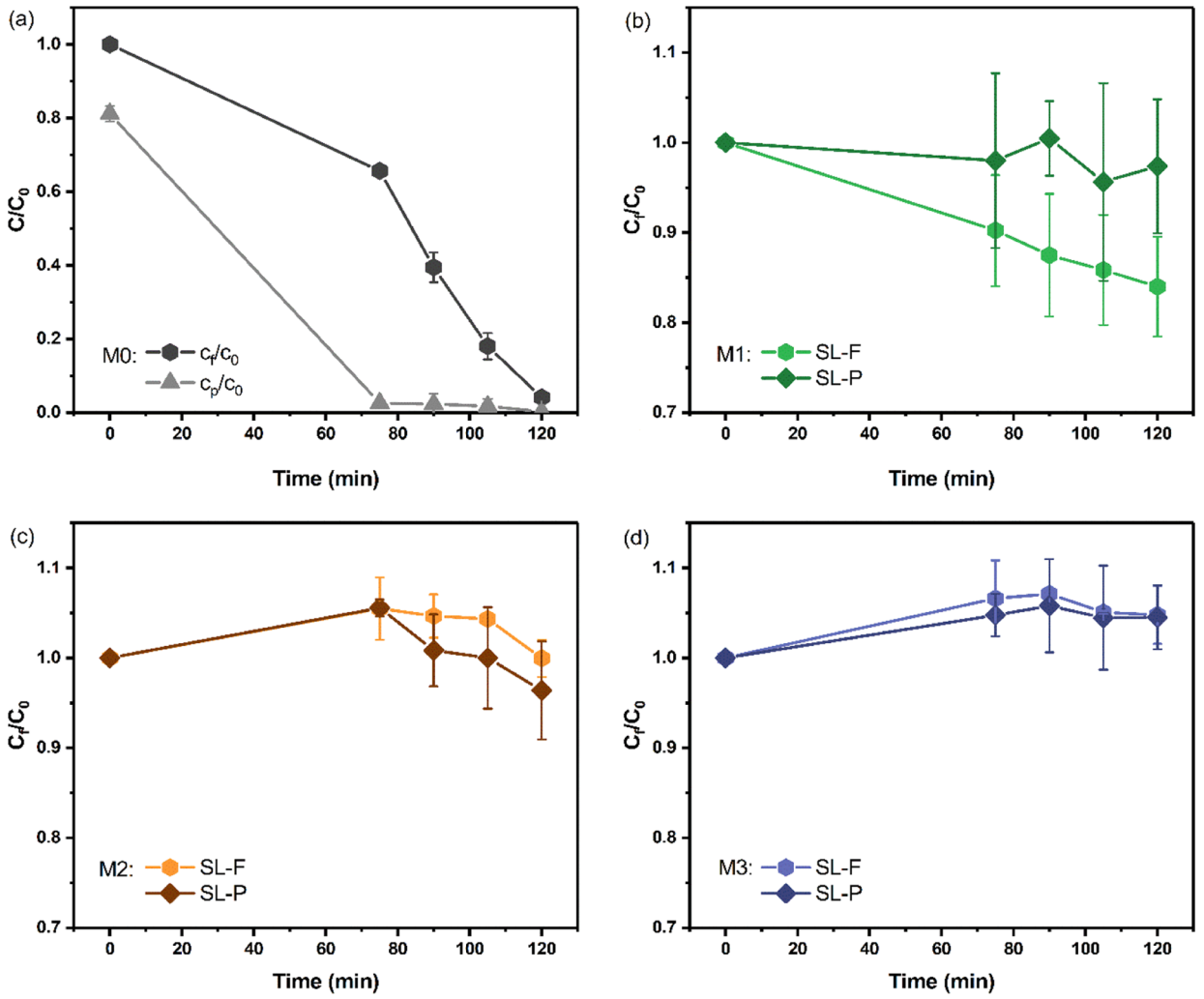

Figure 6. Degradation of naproxen in the feed solution with the double-side-coated membranes: (a) normalized naproxen solution in the feed and permeate when the UF catalytic membranes were measured and the normalized naproxen solution in the feed solution when M1 (b), M_2 (c), and M_3 (d) were measured in both SL-F and SL-P modes. For every data point, three individual membrane samples are measured, and errors are given as the standard deviation.

To explore the degradation efficiency of naproxen in the presence of PMS, the naproxen rejections (here including degradation) were measured after the addition of PMS. As shown in Figure 5b,c, the naproxen rejections all increased after adding PMS, indicating that a catalytic process is effectively combined with membrane separation. In the SL-F mode, M_3 exhibited the highest naproxen rejection after adding PMS (97.2%), showing that higher $R_{PMS/NPX}$ benefits the naproxen degradation in catalytic membranes. Although the improvement of M_3 in naproxen rejection after adding PMS is not the highest among the three types of membranes, considering that it has a very high initial naproxen rejection (77.3 ± 3%) before adding PMS, it is reasonable that we cannot see an absolute improvement that is higher than 23%. However, the rejection of M_2 increased by 40.9% after adding PMS, while the rejection of M_1 only increased by 20.9%, which is different from the trend of the value of $R_{PMS/NPX}$. A possible explanation could be the difference in the surface charge of M_1 and M_2. As shown in Figure S4, the surface of M_1 is more negatively charged compared with that of M_2, probably lowering the accessibility of negatively charged naproxen and HSO_5^- to the catalysts embedded within the porous membranes.[42] In the SL-P mode, M_2 exhibited the highest improvement in naproxen rejection after adding PMS, which corresponds with the value of $R_{PMS/NPX}$. This indicates that similar to the batch experiment, the concentration ratio between oxidants and MPs within the porous catalytic support also exhibits an influence on the degradation efficiency of MPs.

To conclude, the naproxen rejection after adding PMS showed a similar trend as the value of $R_{PMS/NPX}$. Although the concentrations of both naproxen and PMS during the degradation process are under dynamic change, the calculation of the initial concentration ratios of naproxen and PMS in the porous support can still be used as an indicator of the degradation efficiency of naproxen. In the SL-F mode, a higher MP rejection and a lower oxidant rejection benefit the degradation efficiency of naproxen within the porous support. However, considering the molecule size of MPs and oxidants, it is hard to achieve this from only the size-sieving effect. In the SL-P mode, a membrane with lower MP rejection and higher oxidant rejection is favored where the MP degradation can be enhanced due to the higher $R_{PMS/NPX}$. Meanwhile, the surface charge of membranes may affect the accessibility of MPs and oxidants to the catalysts, which still needs further exploration.

https://doi.org/10.1021/acs.iecr.3c00592
Ind. Eng. Chem. Res. 2023, 62, 7622−7634

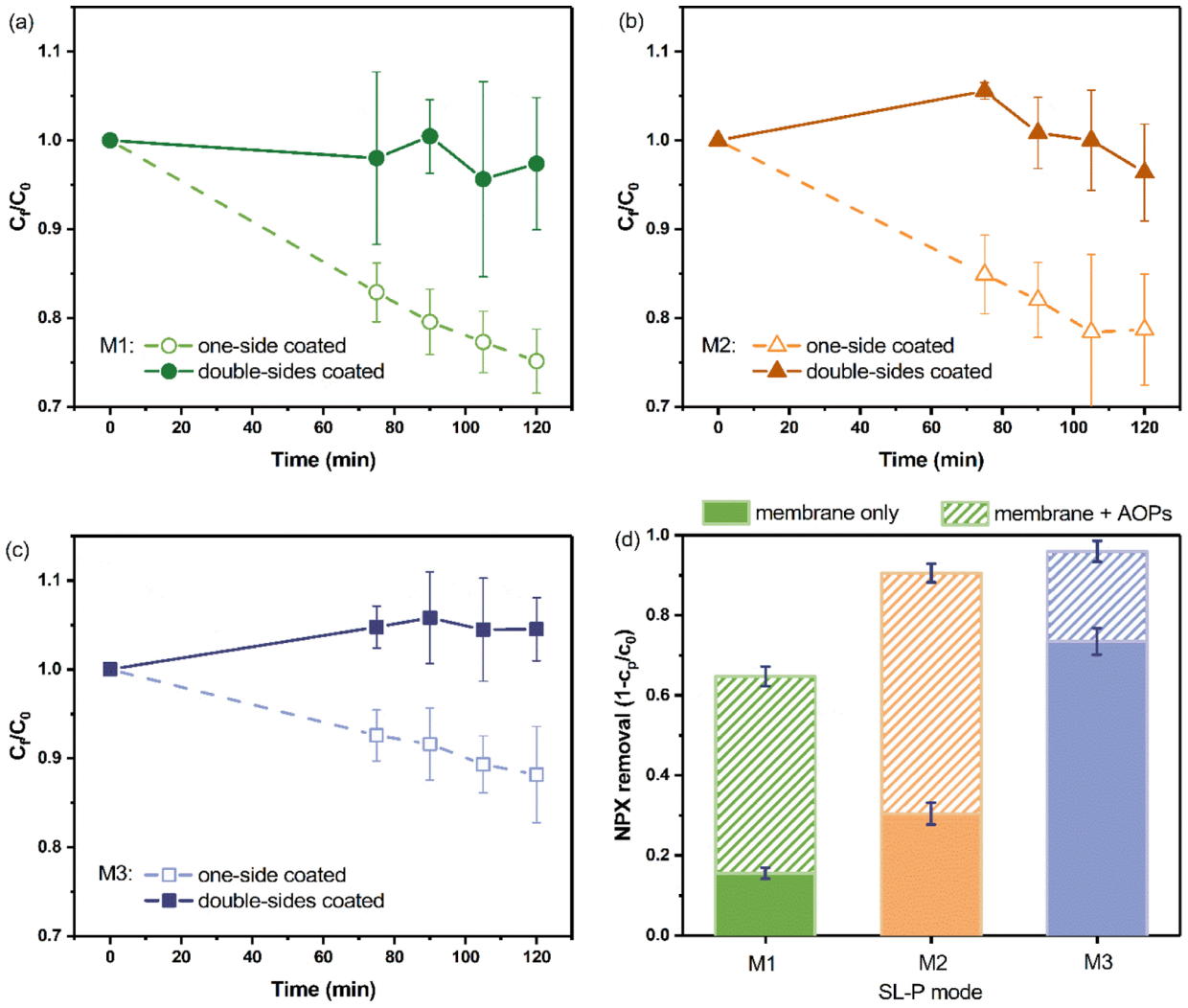

Figure 7. Comparison between dip-coating and one-side-coated membranes on the naproxen degraded in the feed solution: (a) M_1; (b) M_2; (c) M_3; and (d) removal of naproxen when the one-side-coated membranes were measured in the SL-P mode. The pressures applied for one-side-coated membranes were 0.73 ± 0.01 bar, 0.8 ± 0.06 bar, and 0.98 ± 0.06 bar for M_1, M_2, and M_3, respectively. The cross-flow velocity was 0.077 m/s. For every data point, three individual membrane samples are measured, and errors are given as the standard deviation.

Figure 5d illustrates the naproxen removal of different membranes under different membrane orientations. M_3 measured in the SL-F mode exhibited the highest naproxen removal, which is 96.7%. However, it also needs to be emphasized that higher pressure is needed for M_3 to reach the same water flux as M_1 and M_2 due to its denser selectivity layer, which increases its energy cost. Meanwhile, we observed that the removals are slightly different from the rejections, resulting from the fact that the naproxen concentration in the feed solution also changed during the measurement. To further explore the possibility of degrading naproxen in the feed solution, the changes in the naproxen concentration in the feed solution were systematically analyzed in the next section.

4.3. Reducing Naproxen in the Retentate. As elaborated in the introduction, because the porous support membrane directly faces the feed solution, the catalytic membranes in the SL-P mode possess the potential of degrading the concentrated MPs in the feed solution side, which can get rid of the post-treatment of the concentrated retentate. To explore the possibility of this, the concentration changes of the feed solution during the naproxen rejection measurement were monitored. As shown in Figure 6a, the UF catalytic membranes exhibit a super high efficiency of degrading naproxen from both the feed and permeate sides. In 120 min, all the naproxen in the feed solution can be fully degraded, exhibiting the ability to degrade naproxen in the feed solution, while after dip-coating 7.0 bilayers of PDADMAC/PSS polyelectrolytes on both sides of the UF catalytic membranes, as shown in Figure 4b, the degradation in the feed solution dramatically decreased, and only 16% of naproxen in the feed solution can be degraded in the SL-F mode. Moreover, regarding M_2 and M_3, the concentrations of naproxen in the feed solution even increased in 2 h, which can be attributed to the rejection of naproxen. Regardless of membrane orientations, less naproxen can be degraded after coating more bilayers and cross-linking, indicating that the accessibility of PMS and naproxen to the catalysts sharply decreased after the coating of polyelectrolyte multilayers.

To further verify if the coating of polyelectrolytes decreased the naproxen degradation in the feed solution, a one-side coating method was applied to compare with the dip-coating method. As shown in Figure 7a–c, different from the double-side-coated membranes, all the one-side-coated membranes exhibited an improvement in the naproxen removal from the

https://doi.org/10.1021/acs.iecr.3c00592
Ind. Eng. Chem. Res. 2023, 62, 7622−7634

feed solution. Moreover, nearly 30% of naproxen in the feed solution can be degraded when one-side-coated M_1 was used, while only 25 and 15% of naproxen degraded in the feed solution when one-side-coated M_2 and M_3 were applied, respectively, which further shows that the coating of polyelectrolyte bilayers and the cross-linking process make the catalysts within the membrane structure less accessible by naproxen and PMS. The differences in the naproxen degradation efficiency in the feed solution among one-side-coated M_1, M_2, and M_3 also indicate that some polyelectrolytes penetrated through the membrane under gravity, although only one side of the membrane was coated within the homemade setup. It can also be the reason why the naproxen degradation of these one-side-coated membranes in the feed solution is still lower than that of the pristine UF catalytic membranes. Furthermore, the naproxen removal of the one-side-coated membranes was also measured in the SL-P mode. As shown in Figure 7d, the naproxen removals of M_1, M_2, and M_3 are all higher than those of the double-side-coated membranes measured in the SL-P mode (Figure 5d). These results indicate that easy access to naproxen and PMS not only boosts the degradation of naproxen in the feed solution but also the permeate.

5. CONCLUSIONS AND PERSPECTIVES

By careful experiments and the use of concentration polarization models, the effects of membrane orientation on the naproxen degradation efficiency were systematically explored when a selective layer was coated on top of the porous catalytic support membrane. Both the concentration calculations of the oxidant and MPs and the experiment results show that a selective layer with high rejection to MPs and low rejection to the oxidant benefits the degradation of MPs in a separation-catalysis sequence, while it is the opposite in the catalysis-separation sequence. Moreover, it is also demonstrated that the naproxen in the feed solution can be degraded in the catalysis-separation sequence, showing the potential of treating the highly concentrated retentate in the SL-P mode. Meanwhile, the inhibition effect of the polyelectrolyte coating has proven that the accessibility of naproxen and PMS to the catalysts within the polymer matrix decreases after the polyelectrolyte coating. With only one side coated, the membranes exhibited the highest naproxen removal on both the permeate side (97%) and the feed side (12%), which is comparable to the dense reverse osmosis membrane. However, the energy consumption of our catalytic NF membranes is much lower than that of the reverse osmosis process, providing a good option for treating MPs in an energy-efficient way. To conclude, this work compares the performance of dense catalytic membranes under different membrane orientations, giving a comprehensive understanding of the effect of concentration polarization on the treatment efficiency of catalytic NF membranes. More importantly, it also provides valuable information for the design of catalytic membranes with a denser selective layer, where a denser selective layer that can reject both MPs and PMS benefits the performance of catalytic membranes when they are used in the SL-P mode.

To practically apply these catalytic membranes in the treatment of wastewater containing MPs, there are still several studies that need to be done in the future. First, the identification of the byproducts after the catalytic reactions is essential to explore the pathways of the degradation and get the toxicity information of the byproducts. Meanwhile, it is also interesting to check if the selective layer of the catalytic membranes in the SL-P mode can work as a barrier to the byproducts of MPs as well. Second, considering that the hollow fiber nanofiltration membranes based on polyelectrolyte multilayers are already commercially available[34] while the flat sheet membrane structure may limit the large-scale fabrication of these catalytic membranes with the catalytic porous support and polyelectrolyte selective layer, more work can be done to explore the possibility of developing catalytic hollow fiber membranes with such a structure, which would give more insights on the commercial application of these catalytic membranes.

■ ASSOCIATED CONTENT

Supporting Information

The Supporting Information is available free of charge at https://pubs.acs.org/doi/10.1021/acs.iecr.3c00592.

Diffusion coefficient of $MgSO_4$ and naproxen; confidence intervals of B and S with 95% confidence bounds; fluxes of M_1, M_2, and M_3 under different membrane orientations in the naproxen rejection measurement with PMS; calibration curve of PMS concentration measurement; calculation results of naproxen and PMS concentrations of M_1, M_2, and M_3 within the porous catalytic support in both SL-F and SL-P modes; and zeta potential of the front and back surface of M_1, M_2, and M_3 (PDF)

■ AUTHOR INFORMATION

Corresponding Author

Wiebe M. de Vos − *University of Twente, MESA+ Institute for Nanotechnology, Enschede 7500 AE, The Netherlands;* orcid.org/0000-0002-0133-1931; Email: w.m.devos@utwente.nl

Authors

Tao Wang − *University of Twente, MESA+ Institute for Nanotechnology, Enschede 7500 AE, The Netherlands*

Joris de Grooth − *University of Twente, MESA+ Institute for Nanotechnology, Enschede 7500 AE, The Netherlands*

Complete contact information is available at: https://pubs.acs.org/10.1021/acs.iecr.3c00592

Notes

The authors declare no competing financial interest.

■ ACKNOWLEDGMENTS

T.W. received financial support from the China Scholarship Council (CSC PhD fellowship no. 201808440310 to T.W.). The author acknowledges the help from Moritz Junker with the concentration polarization models and Xiaoliu Wen with the drawing of Figure 2. This manuscript was applied as Chapter 4 in the first author's, T.W., PhD thesis ("Catalytic membrane based advanced oxidation processes for micropollutant removal"), and the corresponding Digital Object Identifier (DOI) is https://doi.org/10.3990/1.9789036555371.

■ REFERENCES

(1) Chen, C.; Feng, H.; Deng, Y. Re-Evaluation of Sulfate Radical Based−Advanced Oxidation Processes (SR-AOPs) for Treatment of Raw Municipal Landfill Leachate. *Water Res.* **2019**, *153*, 100−107.

(2) Ao, X.; Liu, W.; Sun, W.; Cai, M.; Ye, Z.; Yang, C.; Lu, Z.; Li, C. Medium Pressure UV-Activated Peroxymonosulfate for Ciprofloxacin Degradation: Kinetics, Mechanism, and Genotoxicity. *Chem. Eng. J.* **2018**, *345*, 87−97.
(3) Oh, W.-D.; Dong, Z.; Lim, T.-T. Generation of Sulfate Radical through Heterogeneous Catalysis for Organic Contaminants Removal: Current Development, Challenges and Prospects. *Appl. Catal., B* **2016**, *194*, 169−201.
(4) Dong, C.; Bao, Y.; Sheng, T.; Yi, Q.; Zhu, Q.; Shen, B.; Xing, M.; Lo, I. M. C.; Zhang, J. Singlet Oxygen Triggered by Robust Bimetallic MoFe/TiO2 Nanospheres of Highly Efficacy in Solar-Light-Driven Peroxymonosulfate Activation for Organic Pollutants Removal. *Appl. Catal., B* **2021**, *286*, 119930.
(5) Duan, X.; Yang, S.; Wacławek, S.; Fang, G.; Xiao, R.; Dionysiou, D. D. Limitations and Prospects of Sulfate-Radical Based Advanced Oxidation Processes. *J. Environ. Chem. Eng.* **2020**, *8*, 103849.
(6) Chen, Z.; Bi, S.; Zhao, G.; Chen, Y.; Hu, Y. Enhanced Degradation of Triclosan by Cobalt Manganese Spinel-Type Oxide Activated Peroxymonosulfate Oxidation Process via Sulfate Radicals and Singlet Oxygen: Mechanisms and Intermediates Identification. *Sci. Total Environ.* **2020**, *711*, 134715.
(7) Giannakis, S.; Lin, K. Y. A.; Ghanbari, F. A Review of the Recent Advances on the Treatment of Industrial Wastewaters by Sulfate Radical-Based Advanced Oxidation Processes (SR-AOPs). *Chem. Eng. J.* **2021**, *406*, 127083.
(8) Zheng, S.; Huang, M.; Sun, S.; Zhao, H.; Meng, L.; Mu, T.; Song, J.; Jiang, N. Synergistic Effect of MIL-88A/g-C3N4 and MoS2 to Construct a Self-Cleaning Multifunctional Electrospun Membrane. *Chem. Eng. J.* **2021**, *421*, 129621.
(9) Yan, H.; Lai, C.; Wang, D.; Liu, S.; Li, X.; Zhou, X.; Yi, H.; Li, B.; Zhang, M.; Li, L.; Liu, X.; Qin, L.; Fu, Y. In Situ Chemical Oxidation: Peroxide or Persulfate Coupled with Membrane Technology for Wastewater Treatment. *J. Mater. Chem. A* **2021**, *9*, 11944−11960.
(10) Wu, L.; Yu, Y.; Zhang, Q.; Hong, J.; Wang, J.; She, Y. A Novel Magnetic Heterogeneous Catalyst Oxygen-Defective CoFe2O4−x for Activating Peroxymonosulfate. *Appl. Surf. Sci.* **2019**, *480*, 717−726.
(11) Li, Y.; Ma, S.; Xu, S.; Fu, H.; Li, Z.; Li, K.; Sheng, K.; Du, J.; Lu, X.; Li, X.; Liu, S. Novel Magnetic Biochar as an Activator for Peroxymonosulfate to Degrade Bisphenol A: Emphasizing the Synergistic Effect between Graphitized Structure and CoFe2O4. *Chem. Eng. J.* **2020**, *387*, 124094.
(12) Tan, C.; Gao, N.; Fu, D.; Deng, J.; Deng, L. Efficient Degradation of Paracetamol with Nanoscaled Magnetic CoFe2O4 and MnFe2O4 as a Heterogeneous Catalyst of Peroxymonosulfate. *Sep. Purif. Technol.* **2017**, *175*, 47−57.
(13) Guo, R.; Li, Y.; Chen, Y.; Liu, Y.; Niu, B.; Gou, J.; Cheng, X. Efficient Degradation of Sulfamethoxazole by CoCu LDH Composite Membrane Activating Peroxymonosulfate with Decreased Metal Ion Leaching. *Chem. Eng. J.* **2021**, *417*, 127887.
(14) Ye, J.; Dai, J.; Li, C.; Yan, Y. Lawn-like Co3O4@N-Doped Carbon-Based Catalytic Self-Cleaning Membrane with Peroxymonosulfate Activation: A Highly Efficient Singlet Oxygen Dominated Process for Sulfamethoxazole Degradation. *Chem. Eng. J.* **2021**, *421*, 127805.
(15) Fan, Y.; Zhou, Y.; Feng, Y.; Wang, P.; Li, X.; Shih, K. Fabrication of Reactive Flat-Sheet Ceramic Membranes for Oxidative Degradation of Ofloxacin by Peroxymonosulfate. *J. Membr. Sci.* **2020**, *611*, 118302.
(16) Wu, H.; Xu, X.; Shi, L.; Yin, Y.; Zhang, L. C.; Wu, Z.; Duan, X.; Wang, S.; Sun, H. Manganese Oxide Integrated Catalytic Ceramic Membrane for Degradation of Organic Pollutants Using Sulfate Radicals. *Water Res.* **2019**, *167*, 115110.
(17) Luo, X.; Liang, H.; Qu, F.; Ding, A.; Cheng, X.; Tang, C. Y.; Li, G. Free-Standing Hierarchical α-MnO2@CuO Membrane for Catalytic Filtration Degradation of Organic Pollutants. *Chemosphere* **2018**, *200*, 237−247.
(18) Westermann, T.; Melin, T. Flow-through Catalytic Membrane Reactors-Principles and Applications. *Chem. Eng. Process.* **2009**, *48*, 17−28.
(19) Wang, T.; de Vos, W. M.; de Grooth, J. CoFe2O4-Peroxymonosulfate Based Catalytic UF and NF Polymeric Membranes for Naproxen Removal: The Role of Residence Time. *J. Membr. Sci.* **2022**, *646*, 120209.
(20) Qing, W.; Li, X.; Shao, S.; Shi, X.; Wang, J.; Feng, Y.; Zhang, W.; Zhang, W. Polymeric Catalytically Active Membranes for Reaction-Separation Coupling: A Review. *J. Membr. Sci.* **2019**, *583*, 118−138.
(21) Nguyen, V. T.; Nguyen, T. B.; Chen, C. W.; Hung, C. M.; Huang, C. P.; Dong, C. D. Cobalt-Impregnated Biochar (Co-SCG) for Heterogeneous Activation of Peroxymonosulfate for Removal of Tetracycline in Water. *Bioresour. Technol.* **2019**, *292*, 121954.
(22) Pang, Y.; Lei, H. Degradation of P-Nitrophenol through Microwave-Assisted Heterogeneous Activation of Peroxymonosulfate by Manganese Ferrite. *Chem. Eng. J.* **2016**, *287*, 585−592.
(23) Gong, C.; Chen, F.; Yang, Q.; Luo, K.; Yao, F.; Wang, S.; Wang, X.; Wu, J.; Li, X.; Wang, D.; Zeng, G. Heterogeneous Activation of Peroxymonosulfate by Fe-Co Layered Doubled Hydroxide for Efficient Catalytic Degradation of Rhoadmine B. *Chem. Eng. J.* **2017**, *321*, 222−232.
(24) McCutcheon, J. R.; Elimelech, M. Influence of Concentrative and Dilutive Internal Concentration Polarization on Flux Behavior in Forward Osmosis. *J. Membr. Sci.* **2006**, *284*, 237−247.
(25) Oh, Y.; Lee, S.; Elimelech, M.; Lee, S.; Hong, S. Effect of Hydraulic Pressure and Membrane Orientation on Water Flux and Reverse Solute Flux in Pressure Assisted Osmosis. *J. Membr. Sci.* **2014**, *465*, 159−166.
(26) Wojcieszyńska, D.; Guzik, U. Naproxen in the Environment: Its Occurrence, Toxicity to Nontarget Organisms and Biodegradation. *Appl. Microbiol. Biotechnol.* **2020**, *104*, 1849−1857.
(27) te Brinke, E.; Achterhuis, I.; Reurink, D. M.; de Grooth, J.; de Vos, W. M. Multiple Approaches to the Buildup of Asymmetric Polyelectrolyte Multilayer Membranes for Efficient Water Purification. *ACS Appl. Polym. Mater.* **2020**, *2*, 715−724.
(28) Mohammad, A. W.; Hilal, N.; Al-Zoubi, H.; Darwish, N. A. Prediction of Permeate Fluxes and Rejections of Highly Concentrated Salts in Nanofiltration Membranes. *J. Membr. Sci.* **2007**, *289*, 40−50.
(29) De, S.; Bhattacharya, P. K. Prediction of Mass-Transfer Coefficient with Suction in the Applications of Reverse Osmosis and Ultrafiltration. *J. Membr. Sci.* **1997**, *128*, 119−131.
(30) Lonsdale, H. K. *Membrane Technology and Applications*; Wiley, 1985; Vol. *23*.
(31) Bui, N. N.; Arena, J. T.; McCutcheon, J. R. Proper Accounting of Mass Transfer Resistances in Forward Osmosis: Improving the Accuracy of Model Predictions of Structural Parameter. *J. Membr. Sci.* **2015**, *492*, 289−302.
(32) Lee, K. L.; Baker, R. W.; Lonsdale, H. K. Membranes for Power Generation by Pressure-Retarded Osmosis. *J. Membr. Sci.* **1981**, *8*, 141−171.
(33) Junker, M. A.; de Vos, W. M.; Lammertink, R. G. H.; de Grooth, J. Bridging the Gap between Lab-Scale and Commercial Dimensions of Hollow Fiber Nanofiltration Membranes. *J. Membr. Sci.* **2021**, *624*, 119100.
(34) Jonkers, W. A.; Cornelissen, E. R.; de Vos, W. M. Hollow Fiber Nanofiltration: From Lab-Scale Research to Full-Scale Applications. *J. Membr. Sci.* **2023**, *669*, 121234.
(35) Zhu, S.; Li, X.; Kang, J.; Duan, X.; Wang, S. Persulfate Activation on Crystallographic Manganese Oxides: Mechanism of Singlet Oxygen Evolution for Nonradical Selective Degradation of Aqueous Contaminants. *Environ. Sci. Technol.* **2019**, *53*, 307−315.
(36) Zhou, Y.; Jiang, J.; Gao, Y.; Ma, J.; Pang, S. Y.; Li, J.; Lu, X. T.; Yuan, L. P. Activation of Peroxymonosulfate by Benzoquinone: A Novel Nonradical Oxidation Process. *Environ. Sci. Technol.* **2015**, *49*, 12941−12950.
(37) Bao, Y.; Lim, T.-T.; Wang, R.; Webster, R. D.; Hu, X. Urea-Assisted One-Step Synthesis of Cobalt Ferrite Impregnated Ceramic Membrane for Sulfamethoxazole Degradation via Peroxymonosulfate Activation. *Chem. Eng. J.* **2018**, *343*, 737−747.

https://doi.org/10.1021/acs.iecr.3c00592
Ind. Eng. Chem. Res. 2023, 62, 7622−7634

(38) Xu, Y.; Ai, J.; Zhang, H. The Mechanism of Degradation of Bisphenol A Using the Magnetically Separable CuFe2O4/Peroxymonosulfate Heterogeneous Oxidation Process. *J. Hazard. Mater.* **2016**, *309*, 87−96.
(39) Liang, C.; Huang, C. F.; Mohanty, N.; Kurakalva, R. M. A Rapid Spectrophotometric Determination of Persulfate Anion in ISCO. *Chemosphere* **2008**, *73*, 1540−1543.
(40) Reurink, D. M.; De Vos, W. M.; Roesink, H. D. W.; De Grooth, J. Polyelectrolyte Multilayers for Forward Osmosis, Combining the Right Multilayer and Draw Solution. *Ind. Eng. Chem. Res.* **2021**, *60*, 7331−7341.
(41) Xu, M.; Li, J.; Yan, Y.; Zhao, X.; Yan, J.; Zhang, Y.; Lai, B.; Chen, X.; Song, L. Catalytic Degradation of Sulfamethoxazole through Peroxymonosulfate Activated with Expanded Graphite Loaded CoFe2O4 Particles. *Chem. Eng. J.* **2019**, *369*, 403−413.
(42) Lotfi, S.; Fischer, K.; Schulze, A.; Schäfer, A. I. Photocatalytic Degradation of Steroid Hormone Micropollutants by TiO2-Coated Polyethersulfone Membranes in a Continuous Flow-through Process. *Nat. Nanotechnol.* **2022**, *17*, 417−423.

https://doi.org/10.1021/acs.iecr.3c00592
Ind. Eng. Chem. Res. 2023, 62, 7622−7634